Available online at www.sciencedirect.com
SCIENCE DIRECT®
Scripta Materialia 55 (2006) 227–230
Scripta MATERIALIA
www.actamat-journals.com

Compressive deformation of a bulk Ce-based metallic glass

J.P. Chu,[a,*] C.L. Chiang,[a] H. Wijaya,[a] R.T. Huang,[a] C.W. Wu,[b]
B. Zhang,[c] W.H. Wang[c] and T.G. Nieh[d]

[a] *Institute of Materials Engineering, National Taiwan Ocean University, Keelung 202, Taiwan, ROC*
[b] *Department of Mechanical and Mechatronic Engineering, National Taiwan Ocean University, Keelung 202, Taiwan, ROC*
[c] *Institute of Physics, Chinese Academy of Science, Beijing 100080, PR China*
[d] *Department of Materials Science and Engineering, The University of Tennessee, Knoxville, TN 37996, USA*

Received 22 February 2006; revised 5 April 2006; accepted 13 April 2006

The compressive deformation behavior of a $Ce_{70}Al_{10}Cu_{20}$ bulk metallic glass at room temperature and in the supercooled liquid region was investigated at strain rates from 8×10^{-4} to $7 \times 10^{-2}\ s^{-1}$. The material exhibited excellent mechanical formability with a high compressive strain of ~89% at $8 \times 10^{-4}\ s^{-1}$ and 420 K. The material could be compressed from a thickness of 1 mm to ~106 μm. Excellent formability in the microscale was demonstrated when the sample was deformed in the supercooled liquid region. The result indicates this alloy is a promising material for fabricating microdevices.

Keywords: Superplasticity; Bulk metallic glass; Compressive behavior; $Ce_{70}Al_{10}Cu_{20}$

When the first amorphous Au–Si ribbon was synthesized by using a rapid quenching method in 1960 [1], it opened a whole new material world. Recent research efforts have made significant progress toward the development of metallic glasses in bulk forms by slow cooling multicomponent alloy systems [2–10]. This class of materials has been generally termed bulk amorphous alloys or bulk metallic glasses (BMG). They exhibit numerous superior properties such as high strength and good fatigue resistance. The deformation of metallic glasses exhibit homogeneous, superplastic behavior in the supercooled liquid region (ΔT) at high temperatures even though they are very brittle at room temperature due to the inhomogeneous deformation behavior. ΔT is conventionally defined as the difference between the glass transition temperature (T_g) and the crystallization temperature (T_x). For instance, previous studies have reported excellent plasticity in bulk Pd- [11–13], Cu- [14,15], and Zr-based [16–22] metallic glasses when deformed in ΔT. Moreover, the deformed behaviors in ΔT exhibited Newtonian and non-Newtonian flows, depending upon the temperature and applied strain rates.

In the present study, the compressive deformation behavior and formability of bulk $Ce_{70}Al_{10}Cu_{20}$ metallic glass in the supercooled liquid region (SLR) were examined. Zhang et al. reported a family of bulk rare-earth Ce-based glassy alloy rods of up to 3 mm in diameter [8–10]. These alloys with a wide SLR and very low T_g show polymer-like thermoplastic behavior. Since the homogeneous deformation of BMGs generally takes place at ~0.8 T_g [23,24], the low T_g might be regarded as an indicator of the ductile character of a BMG, as proposed by Schroers et al. [25]. It is thus of great interest for this study to examine the deformation properties and formability of a Ce-based BMG with low T_g.

A 1 mm-thick Ce-based metallic alloy was cast into a fully glassy plate by a conventional arc-melting method. The nominal alloy composition was determined to be 68.8at.%Ce–10.0%Al–21.2%Cu, using an electron probe microanalyzer. The alloy is hence denoted as $Ce_{70}Al_{10}Cu_{20}$. Compressive specimens with an aspect ratio of 1 were sliced directly from the cast plate. To ensure smooth specimen surfaces, both the top and bottom surfaces were ground with a 1500-grit abrasive paper before testing. The silicon die used for formability evaluation was fabricated by a conventional lithography method consisting of resist spin coating, soft baking, mask alignment, exposure, etching and lift off.

Compressive tests were conducted with a heating furnace-equipped Shimadzu AG250KN Autograph system at room temperature and in a temperature range from

---

[*] Corresponding author. Tel.: +886 2 24622192; fax: +886 2 24625324; e-mail: jpchu@mail.ntou.edu.tw

1359-6462/$ - see front matter © 2006 Acta Materialia Inc. Published by Elsevier Ltd. All rights reserved.
doi:10.1016/j.scriptamat.2006.04.016

400 to 420 K with strain rates from 8×10^{-4} to 7×10^{-2} s^{-1}. A strain-rate-change method was used to determine the strain-rate sensitivity value, m. The glassy state of alloy was examined by X-ray diffractometry (XRD) using monochromatic Cu-Kα radiation ($\lambda = 1.5406$ Å). The glass transition and crystallization behavior were studied using differential scanning calorimetry (DSC) with a heating rate of 40 K/min in Ar. Scanning electron microscopy (SEM) and transmission electron microscopy (TEM) were used for morphology and microstructure analyses.

XRD patterns of the samples tested from 400 to 420 K along with that from the as-cast are shown in Figure 1. Broad Bragg peaks with no detectable crystalline phases are observed in Figure 1. This suggests that the amorphous structure is the major phase in the tested alloys. Thus, the samples are essentially amorphous after testing in the supercooled liquid region. This is consistent with the fact that the deformation time (~10 min) at 420 K is within the incubation period for crystallization, according to the thermal study in Ref. [22]. The inset shows a typical DSC scan of the alloy sample. The T_g and T_x are determined to be 366 K and 427 K, respectively. The supercooled liquid region, ΔT, is 61 K. The enthalpy (ΔH) for crystallization in the as-cast sample is −23.9 J/g. These results are compatible with those reported by Zhang et al. [22]. Figure 2 shows the edge and planar views of bulk $Pd_{40}Ni_{40}P_{20}$ [11], $Cu_{60}Zr_{20}Hf_{10}Ti_{10}$ [14] and $Ce_{70}Al_{10}Cu_{20}$ glasses before and after testing in compression at supercooled liquid region. The Ce-based BMG shows the thickness and compressive strain are 106 μm and 0.89, respectively, at 420 K and 8×10^{-4} s^{-1}. The result indicates this material exhibited excellent deformability in the ΔT. To better describe the formability, Schroers [26] proposed ΔT to be normalized to the width of the undercooled liquid region, $T_l - T_g$, where T_l is the liquidus temperature. Thus, S parameters, which are defined as $\Delta T/(T_l - T_g)$, are calculated for various BMG systems in Table 1, along with thermal properties and formability. It is seen from this table that, in general, a large S is associated with good formability of the BMG. However, from a processing point of view, a low T_g is highly desirable for achieving good formability since it facilitates processing. As demonstrated by Zhang et al., Ce-based BMG also exhibited excellent imprint properties at ~373 K [10].

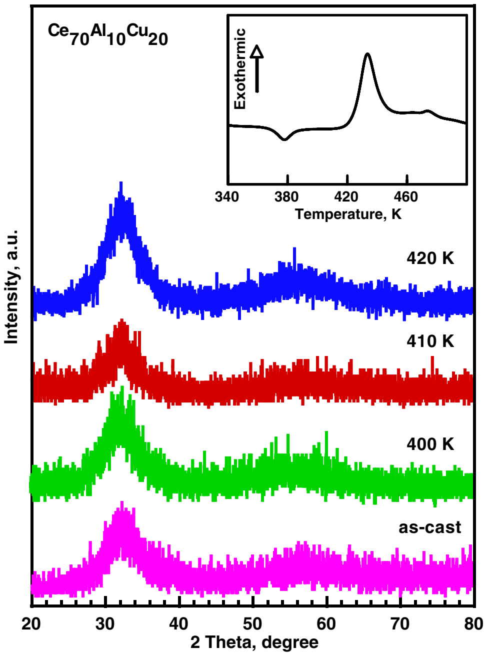

Figure 1. XRD patterns of bulk $Ce_{70}Al_{10}Cu_{20}$ glasses compressive tested at various temperatures. The inset shows the DSC curve at a heating rate of 40 K/min.

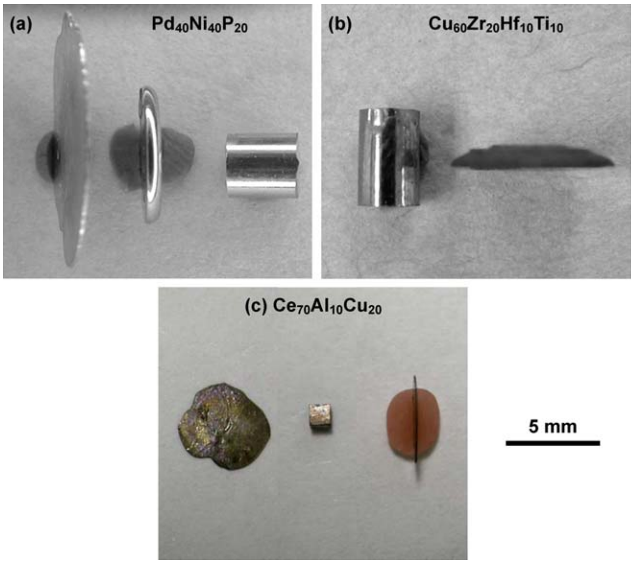

Figure 2. Edge and top views of (a) $Pd_{40}Ni_{40}P_{20}$ [11], (b) $Cu_{60}Zr_{20}Hf_{10}Ti_{10}$ [14] and (c) $Ce_{70}Al_{10}Cu_{20}$ BMG's before and after compression in the supercooled liquid regions.

The relationship between compressive flow stress, viscosity, strain rate sensitivity, and strain rate at various temperatures for the $Ce_{70}Al_{10}Cu_{20}$ glass is shown in Figure 3. Compressive behavior of the bulk $Ce_{70}Al_{10}Cu_{20}$ glass was evidently very sensitive to the test temperature and the applied strain rate. The flow stress is observed to increase with increasing strain rate, and the maximum flow stress is lower than 10 MPa even though at a high strain rate of 7×10^{-2} s^{-1}. For a direct comparison, results from a Pd-based and Cu-based alloy deformed in compression are also included [11,14]. It is noted that flow stresses of the Cu-based glass are about five times higher than those of the Pd-based and Ce-based glass in the ΔT. The Ce-based glass shows the lowest flow stress in the ΔT. Strain rate sensitivity, m, where $m = \Delta \log \sigma / \Delta \log \dot{\varepsilon}$, was measured using a strain rate change method. Variations of strain rate sensitivity (m) and viscosity with strain rate for the $Ce_{70}Al_{10}Cu_{20}$ glass which deformed at 400, 410, and 420 K are shown in Figure 3. It is readily observed that the m value in the ΔT has strong strain-rate dependence; it approaches 1 at low strain rates but decreases rapidly with increasing strain rates in the high strain rate region. The m value is always higher than 0.3 within the strain rate range examined in the present study. Viscosity is calculated using the conventional equation $\eta = \sigma_{\text{flow}}/\dot{\varepsilon}$. In the strain rate region examined, an increase in strain rate leads to a decrease in viscosity. The viscosity varies with

Table 1. Thermal properties and S parameters for various bulk metallic glasses

BMG systems	Thermal properties (K)				$S = \Delta T/(T_l - T_g)$	Formability	References
	T_g	T_x	ΔT	T_l			
$Pd_{40}Ni_{40}P_{20}$	590	671	81	991	0.202	0.94[a]	[11,27]
$Cu_{60}Zr_{20}Hf_{10}Ti_{10}$	760	805	45	1189	0.105	0.77[a]	[14,28]
$Ce_{70}Al_{10}Cu_{20}$	341	408	67	722	0.176	0.89[a]	[10] and present study
$Pt_{57.5}Cu_{14.7}Ni_{5.3}P_{22.5}$	508	606	98	795	0.341	N/A[b]	[26,29]

[a] Compressive strain.

[b] No quantitative data available but it shows good formability according to Ref. [26].

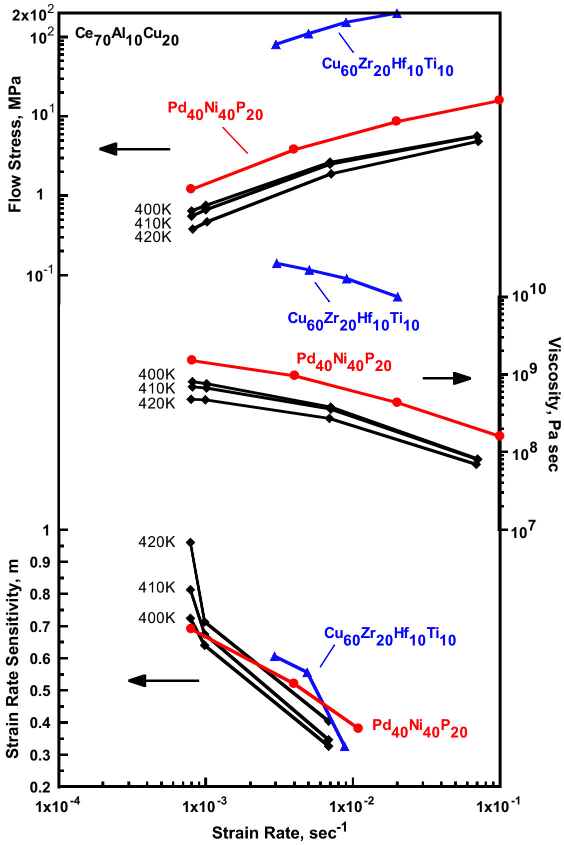

Figure 3. Variations of compressive flow stress, viscosity and strain rate sensitivity (m) with strain rate for samples deformed at 400, 410, and 420 K. Results from $Pd_{40}Ni_{40}P_{20}$ [11] and (b) $Cu_{60}Zr_{20}Hf_{10}Ti_{10}$ [14] BMG's are included for comparisons.

the strain rate, indicating the deformation is changed from Newtonian flow at low strain rates to non-Newtonian flow at high strain rates. It is similar to that of the Pd-based BMG, which shows a distinct transition from Newtonian to non-Newtonian flow [11]. Yet this is different from that of the Cu-based BMG which exhibits a non-Newtonian behavior in the strain-rate range examined. In the present study, both Newtonian and non-Newtonian flows were observed in the Ce-based BMG.

The strain rate–stress relation at various temperatures (400 K, 410 K, and 420 K) can be explained by applying transition state theory, $\dot{\varepsilon} = \dot{\varepsilon}_0 \sinh \frac{\sigma\gamma_0 \Omega_f}{M k_B T}$ where γ_0 is the local strain produced by the shear site of volume Ω_f; k_B, and T have their usual meanings [30–32]. Reger-Leonhard et al. found the Zr-based bulk metallic glass had a linear relationship between strain rate and stress in the low stress regime but transferred to non-linear at high stresses [32].

Despite the difference in the deformation behavior at different strain rates, the $Ce_{70}Al_{10}Cu_{20}$ glasses show large ductility at temperatures in the supercooled liquid region. The superplastic microforming patterns of $Ce_{70}Al_{10}Cu_{20}$ glasses are obtained at 420 K in the ΔT. Deformation at 420 K is in the Newtonian flow region and thus has the best deformability for the bulk metallic glass. It was shown that the highest temperature provides the best formability [26]. The Ce-based alloy is filled fully inside the Si die as shown in Figure 4. The shape of the deformed material duplicates the shape of the Si die. The forming size is from 3 to 75 μm. In summary, the bulk Ce-based metallic glass exhibits superior formability and can be used to fabricate microdevices.

Figure 5(a) shows the TEM image and diffraction pattern of as-cast bulk $Ce_{70}Al_{10}Cu_{20}$ metallic glass. It is a fully amorphous structure of as-cast sample. After processing at 420 K, nanocrystallites are seen in the amorphous matrix, as shown in Figure 5(b). The nanocrystalline phase was predominantly Al_8CeCu_8 as confirmed by the diffraction pattern. DSC was used to evaluate the crystallization effect by measuring the enthalpy of exothermic crystallization peak. Comparison of the enthalpy values of as-cast and tested samples yielded the crystalline volume fraction in the sample. The volume fractions of nanocrystalline phase in samples deformed at 400 and 420 K are estimated to be 3.2% and 14.8%, respectively. Since these crystallites

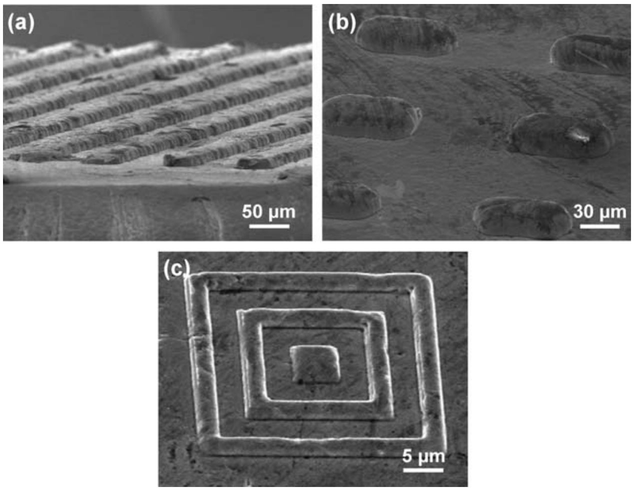

Figure 4. SEM micrographs of various patterns obtained by microforming of bulk $Ce_{70}Al_{10}Cu_{20}$ glasses at 420 K.

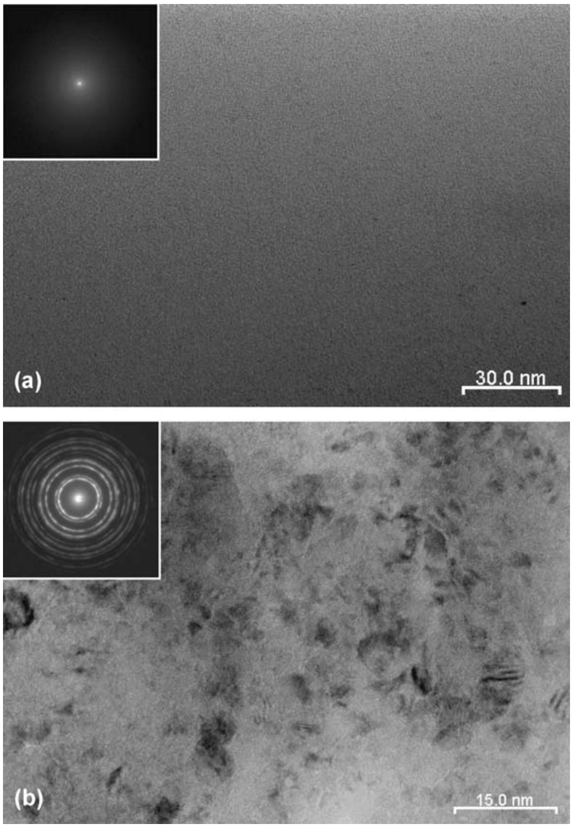

Figure 5. TEM micrographs of bulk $Ce_{70}Al_{10}Cu_{20}$ glasses in (a) as-cast and (b) tested conditions obtained at 420 K. Insets are diffraction patterns taken from each sample.

(in sizes of 20–50 nm) are small with no evidence of apparent grain growth, these crystallites are likely to form in the later stage of compression test. In addition, the compressive strain is 0.89 at 420 K. The formation of crystalline phase presumably has no significant effects on the compressive properties. Similar results have been also reported in the deformation of Pd-based BMG [11].

The excellent plastic deformation behavior of a $Ce_{70}Al_{10}Cu_{20}$ glassy alloy in the supercooled liquid region was demonstrated. A large compressive strain of 0.89 was achieved at 420 K and a strain rate of $8 \times 10^{-4}\ s^{-1}$. The flow stress of the alloy was much lower than those of Pd-based and Cu-based BMGs in their respective supercooled liquid regions. The flow stress increased with increasing strain rate and decreasing temperature. The measured strain rate sensitivity value was approximately 1 at the maximum and decreased to about 0.3 at high strain rates. The low glass transition temperature and large supercooled liquid region were the key factors in the superplastic forming method. This Ce-based metallic glass is expected to be a promising material for microdevices.

The work was supported by the National Science Council of Republic of the China in Taiwan (NSC 94-2120-M-019-001, 93-2216-E-019-007, and 94-2218-E-110-009) and partly supported by Division of Materials Science and Engineering, Office of Basic Energy Sciences, US Department of Energy under contract DE-AC05-00OR-22725 with UT-Battelle.

[1] W. Klement, R.H. Wilens, P. Duwez, Nature 187 (1960) 869.
[2] A. Inoue, H. Yamaguchi, T. Zhang, T. Masumoto, Mater. Trans. JIM 31 (1990) 104.
[3] A. Inoue, T. Nakamura, N. Nishiyama, T. Masumoto, Mater. Trans. JIM 33 (1992) 937.
[4] A. Inoue, A. Kato, T. Zhang, S.G. Kim, T. Masumoto, Mater. Trans. JIM 32 (1991) 609.
[5] A. Inoue, T. Zhang, N. Nishiyama, K. Ohba, T. Masumoto, Mater. Trans. JIM 34 (1993) 1234.
[6] A. Peker, W.L. Johnson, Appl. Phys. Lett. 63 (1993) 2342.
[7] A. Inoue, B. Shen, H. Koshiba, H. Kato, A.R. Yavari, Nature Mater 2 (2003) 661.
[8] B. Zhang, R.J. Wang, D.Q. Zhao, M.X. Pan, W.H. Wang, Phys. Rev. B 70 (2004) 224208.
[9] B. Zhang, M.X. Pan, D.Q. Zhao, W.H. Wang, Appl. Phys. Lett. 85 (2004) 61.
[10] B. Zhang, D.Q. Zhao, M.X. Pan, W.H. Wang, A.L. Greer, Phys. Rev. Lett. 94 (2005) 205502.
[11] J.P. Chu, C.L. Chiang, T.G. Nieh, Y. Kawamura, Intermetallics 10 (2002) 1191.
[12] Y. Saotome, K. Itoh, T. Zhang, A. Inoue, Scripta Mater. 44 (2001) 1541.
[13] Y. Kawamura, T. Nakamura, A. Inoue, Scripta Mater. 39 (1998) 301.
[14] C.L. Chiang, J.P. Chu, C.T. Lo, T.G. Nieh, Z.X. Wang, W.H. Wang, Intermetallics 12 (2004) 1057.
[15] D.H. Bae, H.K. Lim, S.H. Kim, D.H. Kim, W.T. Kim, Acta Mater. 50 (2002) 1749.
[16] J.P. Chu, C.L. Chiang, T. Mahalingam, T.G. Nieh, Scripta Mater. 49 (2003) 435.
[17] W.J. Kim, D.S. Ma, H.G. Jeong, Scripta Mater. 49 (2003) 1067.
[18] G. Wang, J. Shen, J.F. Sun, Y.J. Huang, J. Zou, Z.P. Lu, Z.H. Stachurski, B.D. Zhou, J. Non-Cryst. Solids 351 (2005) 209.
[19] J. Lu, G. Ravichandran, W.L. Johnson, Acta Mater. 51 (2003) 3429.
[20] K.S. Lee, T.K. Ha, S. Ahn, Y.W. Chang, J. Non-Cryst. Solids 317 (2003) 193.
[21] Y. Kawamura, T. Shibata, A. Inoue, T. Masumoto, Scripta Mater. 37 (1997) 431.
[22] T.G. Nieh, T. Mukai, C.T. Liu, J. Wadsworth, Scripta Mater. 40 (1999) 1021.
[23] A.S. Argon, Acta Metall. 27 (1979) 47.
[24] P. Wesseling, T.G. Nieh, W.H. Wang, J.J. Lewandowski, Scripta Mater. 51 (2004) 151.
[25] J. Schroers, W.L. Johnson, Phys. Rev. Lett. 93 (2004) 255506.
[26] J. Schroers, JOM 35 (May) (2005).
[27] A. Inoue, N. Nishiyama, H. Kimura, Mater. Trans. JIM 38 (1993) 179.
[28] Z.X. Wang, D.Q. Zhao, M.X. Pan, W.H. Wang, T. Okada, W. Utsumi, J. Phys. Condens. Mater 15 (2003) 5923.
[29] J. Schroers, W.L. Johnson, Appl. Phys. Lett. 84 (2004) 18.
[30] A.I. Taub, Acta Metall. 28 (1980) 633.
[31] A.I. Taub, F.E. Luborsky, Acta Metall. 29 (1981) 1939.
[32] A. Reger-Leonhard, M. Heilmaier, J. Eckert, Scripta Mater. 43 (2000) 459.